Specificity Determinants in Small Multidrug Transporters

Shlomo Brill, Ofir Sade-Falk[1], Yael Elbaz-Alon[2] and Shimon Schuldiner

Department of Biological Chemistry, *Alexander Silberman Institute of Life Sciences, Hebrew University of Jerusalem, 91904 Jerusalem, Israel*

Correspondence to Shimon Schuldiner: *shimon.schuldiner@huji.ac.il.*
http://dx.doi.org/10.1016/j.jmb.2014.11.015
Edited by I. B. Holland

Abstract

Multiple-antibiotic resistance has become a major global public health concern, and to overcome this problem, it is necessary to understand the resistance mechanisms that allow survival of the microorganisms at the molecular level. One mechanism responsible for such resistance involves active removal of the antibiotic from the pathogen cell by MDTs (*m*ulti*d*rug *t*ransporters). A prominent MDT feature is their high polyspecificity allowing for a single transporter to confer resistance against a range of drugs. Here we present the molecular mechanism underlying substrate recognition in EmrE, a small MDT from *Escherichia coli*. EmrE is known to have a substrate preference for aromatic, cationic compounds, such as methyl viologen (MV^{2+}). In this work, we use a combined bioinformatic and biochemical approach to identify one of the major molecular determinants involved in MV^{2+} transport and resistance. Replacement of an Ala residue with Ser in weakly resistant SMRs from *Bacillus pertussis* and *Mycobacterium tuberculosis* enables them to provide robust resistance to MV^{2+} and to transport MV^{2+} and has negligible effects on the interaction with other substrates. This shows that the residue identified herein is uniquely positioned in the binding site so as to be exclusively involved in the mediating of MV^{2+} transport and resistance, both in EmrE and in other homologues. This work provides clues toward uncovering how specificity is achieved within the binding pocket of a polyspecific transporter that may open new possibilities as to how these transporters can be manipulated to bind a designed set of drugs.

Introduction

The antibiotic revolution has saved millions of lives from infectious diseases. However, only a little more than half a century later, antibiotic resistance has become a global public health concern [1–3]. Microorganisms have developed resistance that limits therapeutic options and drives clinicians to use newer and more expensive agents. In extreme cases, multiple resistance to various antibiotics leaves no treatment options. The pipeline of new antibiotics in development is very limited because of the costs involved and the low return on investment relative to the development of other therapeutic classes of drugs. In addition, the lifetime of new antibiotics is very short because of the advent of novel resistance mechanisms.

One of the strategies to deal with this problem is to understand the resistance mechanisms that allow survival of the microorganisms. One of such mechanisms involves active removal of the antibiotic from the cell by transporters [4–6]. These are membrane proteins (MDTs, *m*ulti*d*rug *t*ransporters) that recognize a wide range of antibiotics, remove them from the cell in an energy-dependent process and are responsible for the resistance in some microorganisms. Understanding their mechanism at the molecular level will contribute to develop strategies to combat a phenomenon that poses a serious problem in the treatment of infectious diseases.

A salient feature of the MDTs is their high polyspecificity. Some of the MDTs have been reported to confer resistance to dozens of toxic compounds that apparently posses few common features [7–12]. Understanding the molecular mechanism of recognition of such a wide variety of substrates necessitates a combined structural and biochemical approach.

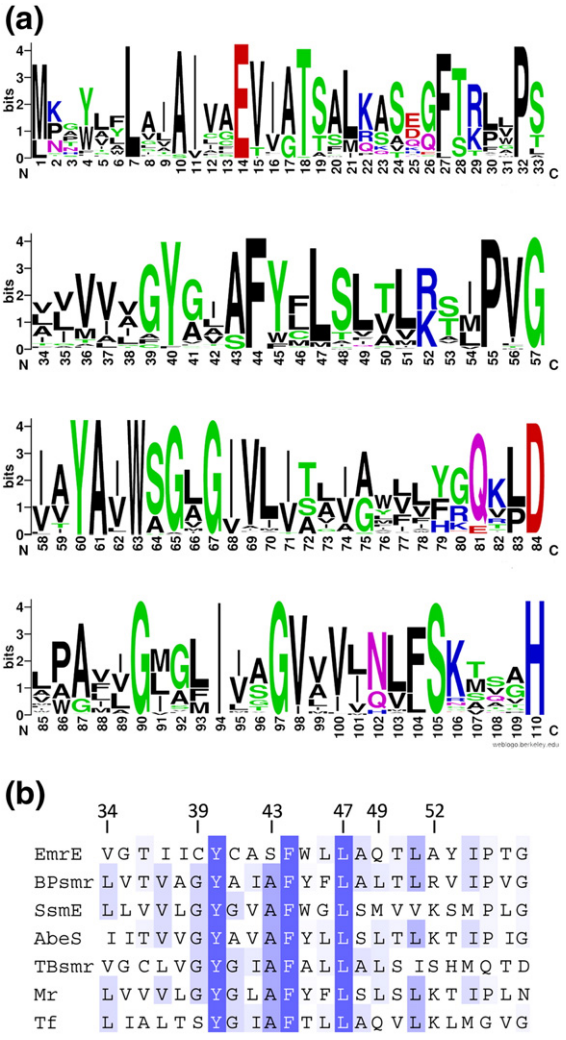

Fig. 1. Multiple sequence alignment of members of the SMR family. Sequence conservation analysis was performed as described in Materials and Methods. The height of the letters in the logo show the probability of each amino acid type in EmrE after multiple sequence alignment of 369 EmrE homologues, colored for acidic (red), basic (blue), small or polar (green), or other residue types (black). Logos were made by including only the homologues that are less than 50% similar to wild-type EmrE. Logos were generated using WebLogo v3.3.

In *Escherichia coli* and other Gram-negative bacteria, the AcrAB-TolC complex is thought to be the major multidrug efflux system [13]. Extensive structural studies of this complex reveal a large substrate binding cavity and a variety of binding determinants [10,11]. This complex removes toxicants and antibiotics from the periplasmic space and/or from the outer leaflet of the cytoplasmic membrane. Removal of its substrates from the cytoplasm necessitates collaboration with other MDTs such as EmrE and MdfA [14]. The efflux activity by the MDT cohort provides a significant challenge to antimicrobial therapy that warrants closer study of such proteins.

EmrE is the most well-studied member of the SMR (*s*mall *m*ultidrug *r*esistance) family to date, as it is an excellent paradigm for the study of H^+ antiporters [15]. EmrE has a well-documented substrate preference for aromatic cations, among them is the divalent methyl viologen (MV^{2+}) [16]. Among the SMR proteins, robust MV^{2+} resistance and transport has been shown both *in vivo* and *in vitro* [16] only for EmrE. Furthermore, experiments with EmrE homologues have shown that this is not a universal feature of the SMR family. Here we report the use of a combined biochemical and bioinformatic approach to identify a key residue essential for transport of MV^{2+}. Comparison of the sequences of EmrE and other SMRs that have been shown to confer weak or nil resistance to MV^{2+} revealed the identity of Ser43 in TM2 in EmrE as a potentially important residue. Replacement of the corresponding alanine residue with serine in two different homologues of EmrE enables them to provide robust resistance to MV^{2+} *in vivo* and to transport MV^{2+} as determined in proteoliposome assays. We conclude that a Ser residue at this position is a critical determinant for MV^{2+} recognition and transport.

Results

Position Ser43 in EmrE is a major MV^{2+} resistance determinant

While most SMR transporters thus far characterized transport monovalent substrates such as ethidium and acriflavine, bacterial homologues from *Mycobacterium tuberculosis* (TBsmr), *Bordetella pertusis* (BPsmr) and *Serratia marcescens* (SsmE) [27] and the archaeal homologue Hsmr confer marginal or nil MV^{2+} resistance *in vivo* [20,28]. EmrE homologues from *Meiothermus ruber* (MrSMR) and *Thermobifida fusca* (TfSMR) showed MV^{2+} resistance *in vivo*, but no *in vitro* activity was detectable [29], implying that the resistance may not be directly linked to MV^{2+} transport.

The binding determinants that are involved in MV^{2+} resistance have so far remained elusive. Previous studies have shown that mutations in TM2 alter substrate specificity such as mutation of the highly conserved Leu47 residue to Phe, which is resistant to acriflavine and ethidium but partially loses its ability to confer resistance to MV^{2+} [25]. Cysteine scanning of TM2 has found that a number of residues in TM2 appear to be involved in MV^{2+} resistance, including Val34, Ala48 and Ala52 [30]. Sequence conservation analysis (Fig. 1a) reveals that, while Leu47 is fully conserved, the others (Val34, Ala48 and Ala52) are not, implying that residue conservation is not necessarily an absolute indicator of a potential MV^{2+} resistance determinant. Indeed, mutation of the highly

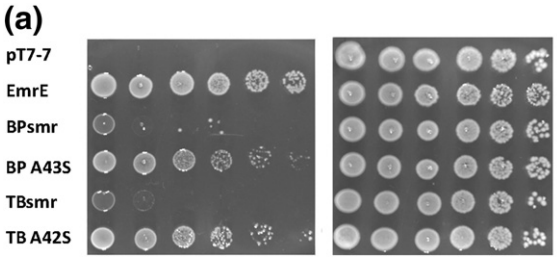

(b)

Protein	IC_{50}
pT7-7	7.1 μM ± 0.4
EmrE	44.3 μM ± 0.9
BPsmr	18.6 μM ± 0.7
BP A43S	52.2 μM ± 5
TBsmr	14.5 μM ± 0.6
TB A42S	43.3 μM ± 6.6

Fig. 2. BP A43S and TB A42S mutants confer resistance to MV^{2+}. (a) *E. coli* DH5α cells transformed with pT7-7 (vector), pT7-7-EmrE or pT7-7 with each of the mutants were grown overnight at 37 °C in LB medium containing ampicillin. We spotted 5 μl of serial dilutions of the culture onto LB plates containing 30 mM BTP (pH 7.0), with (left panel) or without (right panel) the addition of 0.4 mM MV^{2+}. Growth was analyzed after an overnight incubation at 37 °C. (b) Cells were grown to mid-logarithmic phase and diluted to a final OD_{600} of 0.01 with a broad range of MV^{2+} concentrations at 37 °C and their OD_{600} was measured at hourly intervals using a Synergy 2 BioTek Microplate Reader. IC_{50} values were calculated by comparing growth of each mutant at mid-log phase, using non-linear regression software Origin 8.6 (OriginLab).

conserved Tyr40 yielded no effect on MV^{2+} resistance yet caused a total loss of resistance to both of the other well-characterized substrates (ethidium and acriflavine) [31].

Since the modification of a significant number of residues in TM2 results in altered substrate specificity, including MV^{2+} resistance, and the major resistance determinants seem to be found in TM2, we focused our studies on this domain. Sequence alignment of TM2 of seven SMRs that have been studied by us and others [27,29,32] in some detail is shown in Fig. 1b. To our knowledge and as already mentioned above, EmrE is the only one that was shown to confer robust resistance to MV^{2+} *in vivo* and to mediate H^+-dependent antiport activity *in vitro*. A striking correlation is revealed between MV^{2+} resistance and the presence of serine at position 43 of EmrE (Fig. 1b). Sequence conservation analysis shows that position 43 of EmrE predominantly has either Ala or Ser (Fig. 1a). Further analysis of the alignment shows that this position is Ser in EmrE and Ala in non-resistant homologues, implying that this could be an amino acid involved in the resistance of EmrE to MV^{2+}.

Replacement of Ala with Ser makes sensitive homologues resistant to MV^{2+}

Based on the reasoning mentioned above, we tested whether replacement of the Ala residue with Ser in two strains that confer weak resistance modifies their specificity. The result of such a replacement in TBsmr and BPsmr (A42S and A43S, respectively) is shown in Fig. 2. In these experiments, the ability of cells transformed with plasmids coding for wild-type EmrE and wild-type and mutated TBsmr and BPsmr to grow in the presence of MV^{2+} was analyzed. In Fig. 2a, 5 μl of a series of 10-fold dilutions was spotted on LB plates with (left) or without (right) the addition of MV^{2+} at a concentration (0.4 mM) that prevents growth of cells mock-transformed with a plasmid that carries no SMR gene (pT7-7). Cells expressing wild-type EmrE show robust growth even at the highest dilutions while those expressing BPsmr or TBsmr showed only a very weak growth. Strikingly, however, a single mutation from Ala to Ser allowed for growth of the mutants almost as robust as detected with EmrE. IC_{50} values were estimated from the ability of cells to grow in liquid media in the presence of a range of MV^{2+} concentrations (Fig. 2b). While IC_{50} values in cells expressing EmrE were 6- to 7-fold higher than those mock-transformed, cells transformed with BPsmr or TBsmr showed only about a 2-fold increase. Strikingly, cells expressing the single mutants A43S and A42S, respectively, displayed IC_{50} values comparable to those of EmrE, 6- to 7-fold higher than mock-transformed cells.

BPsmr A43S and TBsmr A42S mutants transport MV^{2+} in proteoliposomes

To test whether the phenomenon observed in the phenotype assays is due to the protein in question, we purified the wild-type and mutant proteins, reconstituted them into proteoliposomes and evaluated them for their ability to transport MV^{2+} (Fig. 3). For this purpose, we over-expressed proteins 6×His-tagged at the C-terminus, purified them with immobilized metal affinity chromatography and reconstituted them into proteoliposomes. To generate a pH gradient, we loaded the proteoliposomes with $(NH_4)_2SO_4$ and diluted them into an ammonium-free buffer. A proton gradient (acidic inside) was generated upon dilution that drove substantial $[^{14}C]MV^{2+}$ accumulation in proteoliposomes containing EmrE (Fig. 3a) but only marginally in BPsmr (Fig. 3b) and TBsmr proteoliposomes (Fig. 3c). Reconstitution of the EmrE S43A mutant shows that MV^{2+} transport has been severely compromised (Fig. 3a) while the Ala → Ser replacements in BPsmr and TBsmr gain the ability to transport MV^{2+} to significant levels. An analysis of the kinetic parameters of the transport reaction revealed that the BP A43S mutant has a V_{max} of 23.2 nMoles MV^{2+} per

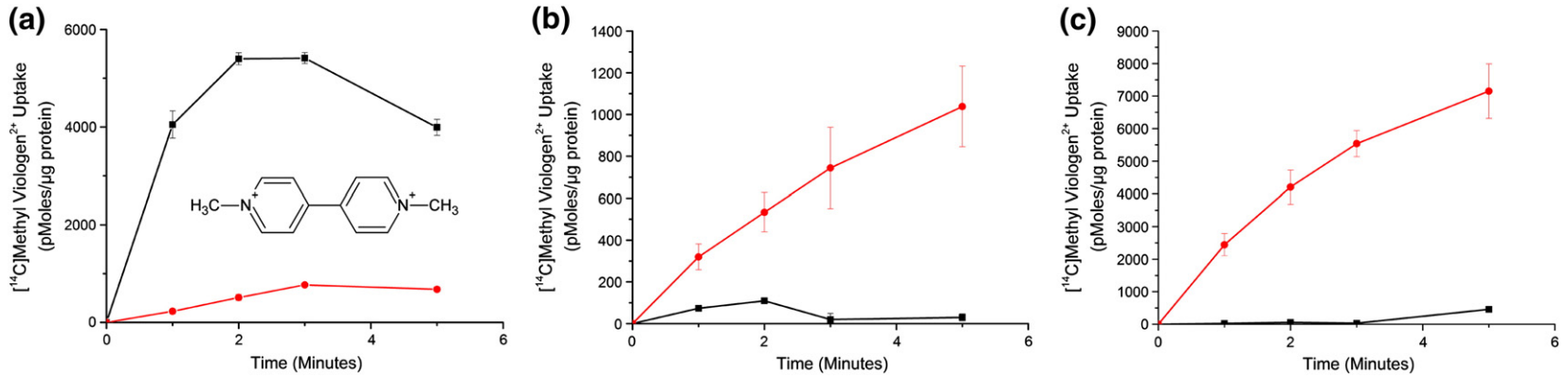

Fig. 3. BP A43S and TB A42S mutants transport MV^{2+}. Proteoliposomes reconstituted with each of the purified proteins and loaded with NH_4Cl were diluted into an ammonium-free medium and transport was measured over the stated time intervals, as described in Materials and Methods. A 5-min time point with nigericin (an ionophore that destroys the proton gradient) was subtracted from each point of the time course. (a) Black, EmrE; red, EmrE S43A. The molecular structure of MV^{2+} is shown in the inset. (b) Black, BPsmr; red, BP A43S. (c) Black, TBsmr; red, TB A42S.

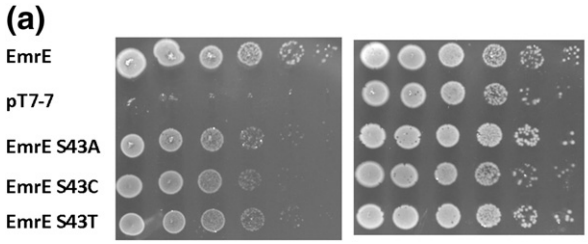

(b)

Protein	IC_{50}
EmrE S43A	26.3 μM ± 2.3
EmrE S43C	23.1 μM ± 1.2
EmrE S43T	23.2 μM ± 1.3

Fig. 4. Ser43 is an essential but not unique determinant of MV^{2+} specificity. (a) Resistance of *E. coli* DH5α cells transformed with pT7-7 (vector), pT7-7-EmrE or pT7-7 with each of the mutants was assayed as described in Fig. 2 on LB plates with (left panel) or without (right panel) the addition of 0.4 mM MV^{2+}. (b) IC_{50} values were calculated as described in Fig. 2.

microgram of protein per minute (compared with a value of 0.4 nMoles MV^{2+} per microgram of protein per minute for the wild-type protein [20]) with a K_m of 2.1 mM and the TB A42S mutant has a V_{max} of 150 nMoles MV^{2+} per microgram of protein per minute (compared with a value of 22 nMoles MV^{2+} per microgram of protein per minute for the wild-type protein [20]) with a K_m of 795 μM.

Ser43 is an essential determinant but not a unique one

As shown above, replacement of Ser43 in EmrE with Ala resulted in a dramatically lower but still detectable transport rate. The rate was too slow to allow for determination of the kinetic parameters. The mutant was capable of conferring a weak but noticeable resistance to MV^{2+} as judged by growth on solid medium (Fig. 4a, left panel) and by the IC_{50} values (26.3 μM). The EmrE S43A, S43C and S43T mutants displayed very similar phenotypes suggesting that Ser at this position is irreplaceable for high rates and robust resistance. However, low transport rates and medium-to-low resistance are supported by the three substitutions at this position and also, albeit to a lower degree, by wild-type BPsmr and TBsmr as shown by their IC_{50} values compared to that of the vector alone (Fig. 2b).

Recognition of other substrates is minimally affected by the mutations

To test whether the Ser43 position is also an important determinant for substrates other than MV^{2+}, we tested the effect of the mutations described above for the well-characterized substrates tetraphenylphosphonium (TPP^+) and 1-methyl-4-phenylpyridinium (MPP^+). For this purpose, transport of MPP^+ was assayed with the proteoliposomes described above. As can be seen from Fig. 5, the impact of the Ala-to-Ser mutation in the EmrE homologues is minimal (at most 1.5-fold). When examining the EmrE S43A mutant, the change in MPP^+ transport is slightly higher and accounts for a stimulation of about 3-fold in the rate. These results show that this position has relatively little effect on MPP^+ transport when compared to the increase of circa 3 orders of magnitude seen for MV^{2+} in the homologues.

All of the aforementioned proteins were also assayed for TPP^+ binding, a high-affinity substrate of several SMR transporters. Figure 6 shows that the Ala-to-Ser mutation made in the EmrE homologues resulted in a change that was at about 3-fold and the EmrE S43A mutation resulted in a 1.2-fold difference in TPP^+ binding. These results show that the involvement of the Ser43 position in TPP^+ binding is marginal at best.

Discussion

The dearth of high-resolution structural information in the SMR family and the ongoing controversy on the relative topology of the protomers in the EmrE homodimer led us to expand our biochemical studies to understand the broad specificity of EmrE, the best-studied SMR transporter. Two structural models that are available at the time of writing this manuscript provide us only with a very low-resolution view of the EmrE dimer [33,34]. Furthermore, the model provides a view of only one of the topoforms of EmrE [35]. We focused our studies on the transport of MV^{2+} because, to our knowledge, EmrE is the only SMR homodimer that has been reported to confer robust resistance to MV^{2+} as assayed *in vivo* and shown to transport in an *in vitro* assay using purified protein reconstituted in proteoliposomes. Interestingly, some homologues have been reported to confer some resistance *in vivo*, but weak [20] or no *in vitro* activity was detectable [29], implying that the resistance may not be directly linked to MV^{2+} transport. A heterodimeric SMR from *Bacillus subtilis* has been reported to confer an extremely robust resistance to MV^{2+} but *in vitro* transport activity was not recounted [36]. In addition, MV^{2+} is quite unique among SMR substrates because it is divalent, relatively hydrophilic and is not transported by the AcrAB-TolC complex [14].

As already discussed above, there have been numerous reports that mutation of certain residues in

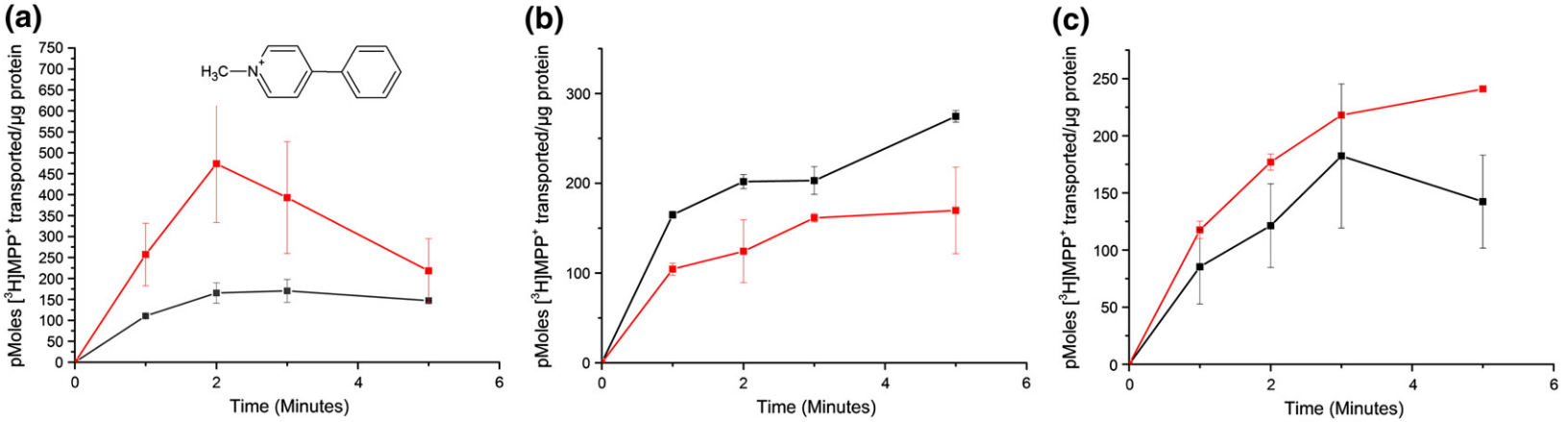

Fig. 5. BP A43S, TB A42S and EmrE S43A mutations have a relatively minor impact on MPP^+ transport in proteoliposomes. Ammonium-loaded proteoliposomes reconstituted with each of the purified proteins were diluted into an ammonium-free medium with 1 µM [^{3}H]MPP^+ and transport was measured over the stated time intervals, as described in Materials and Methods. A 5-min time point with nigericin was subtracted from each point of the time course. (a) Black, EmrE; red, EmrE S43A. The molecular structure of MPP^+ is shown in the inset. (b) Black, BPsmr; red, BP A43S. (c) Black, TBsmr; red, TB A42S.

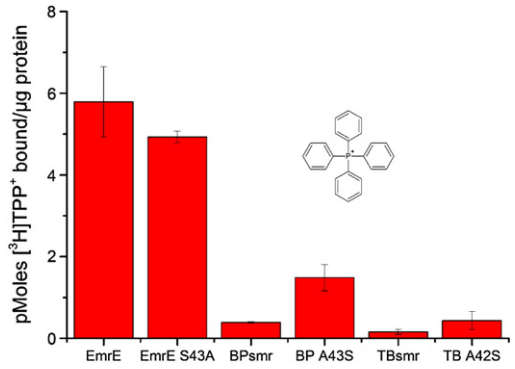

Fig. 6. BP A43S, TB A42S and EmrE S43A mutations have a relatively minor impact on TPP^+ binding in detergent solubilized protein. TPP^+ binding was performed essentially as described in Materials and Methods. The molecular structure of TPP^+ is shown in the inset.

TM2 has a significant impact on substrate selectivity and resistance. As seen in the helical projection of TM2 (Fig. 7), the identified residues cluster on two subdomains of the helix. We speculate that one of them, the one that includes residues Tyr40, Ser43 and Leu47, is the side that faces the substrate binding cavity and/or pathway. The other subdomain that includes Val34, Ala48 and Ala52 may be interacting with other transmembrane domains and indirectly affecting specificity.

Analysis of a multiple sequence alignment of EmrE homologues whose MV^{2+} resistance has been characterized threw up the possibility that Ser43 could be involved in MV^{2+} resistance, as resistant

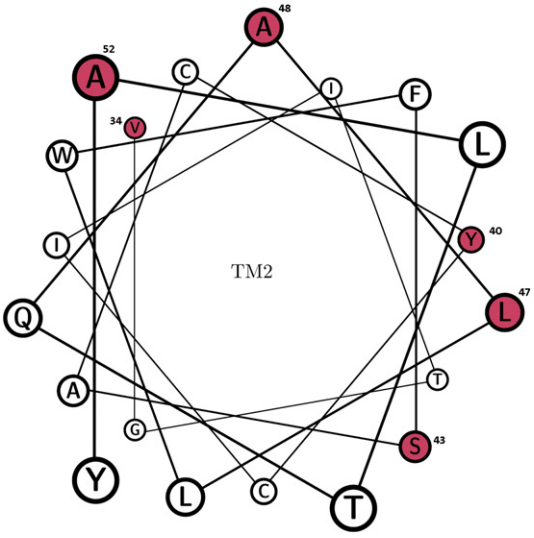

Fig. 7. Helical wheel projection of TM2 of EmrE. In addition to Ser43 described here, the other residues highlighted were studied in Refs. [25], [30] and [31].

proteins bear a serine at this position and sensitive proteins have an alanine. After having identified Ser43 as a potentially interesting residue to explore, mutation of this amino acid to serine in MV^{2+}-sensitive EmrE homologues BPsmr and TBsmr results in a clear and convincing resistance as shown by the plate phenotype and the IC_{50} value of each strain, thereby implying that this position is directly involved in MV^{2+} resistance. This is further supported by the *in vitro* transport data, where the mutants display increased MV^{2+} transport by several orders of magnitude. Mutating Ser43 to Ala, Cys or Thr resulted in a compromised yet not entirely eliminated resistance. This implies that it is not sufficient to have a polar or very similar residue at this position; the spatial positioning of the residue seems to be of utmost importance for maximal effect. Although essential for maximal effect, Ser43 is not the only determinant as suggested by the fact that Ala replacements in EmrE and the original wild-type BPsmr and TBsmr can still provide a weak resistance and a very low but detectable transport. Moreover, Ser43 is not sufficient by itself since Hsmr, a homologue from *Halobacterium sp. NRC-1* displays no detectable resistance and transport but has a Ser at position 43 [28].

To evaluate the effect of the EmrE S43A mutation and the converse mutations in the EmrE homologues on the ability to recognize and transport other substrates, we examined TPP^+ binding and MPP^+ transport. The changes of TPP^+ binding and MPP^+ transport as a result of the mutations are relatively modest implying that Ser43 may be a specific determinant for recognition of MV^{2+}. This conclusion is in line with the suggestion that recognition of a large number of substrates is possible because of the existence of multiple determinants in a relatively large cavity [37–40].

The results described in this work provide biochemical information on the specificity determinant for MV^{2+} in SMR transporters. The outstanding question of what the remaining determinants are is a conundrum that has yet to be resolved and further work and high-resolution structural information are needed to provide answers to this question.

Materials and Methods

Plasmids and strains

In this work, *E. coli* DH5α (Invitrogen) and TA15 [17] were used. All genes were cloned into the pT7-7 vector [18] and tagged with a Myc epitope followed by a hexa-His tag at their C-terminus as previously described for EmrE [19]. The transporters from *M. tuberculosis* (TBsmr, UniProt accession number: W6GRR5) and from *Bacillus pertussis* (BPsmr, UniProt accession number: Q7VW02) were cloned and partially characterized in reference [20].

Sequence conservation analysis

Five iterations of PSI-BLAST [21] searches were conducted using the EmrE protein sequence on August 1, 2014. Apart from using the BLOSUM45 matrix and retrieving 1000 sequences, we maintained all the default settings. Between each iteration, sequences that were duplicates of EmrE were removed before using the results for the next iteration. The final set of sequences obtained after the fifth iteration were aligned using the COBALT alignment tool. From this alignment, sequences with a similarity above 50% were removed, resulting in a final alignment of 369 homologues, each bearing no less similarity than 36.3%. The WebLogo [22,23] server was then used to generate the final conservation analysis representation.

Resistance to toxic compounds

For testing resistance on solid medium, *E. coli* DH5α cells were transformed with the indicated plasmid and were grown overnight at 37 °C in LB medium with the corresponding antibiotic. The cultures were diluted to A_{600} = 0.5 and 5 µl of serial dilutions of the culture was spotted on LB plates containing 30 mM 1,3-bis[tris(hydroxymethyl)methylamino]propane (BTP), pH 7.0, with or without the addition of the indicated concentrations of MV^{2+}. Growth was visualized after overnight incubation at 37 °C. Methyl viologen (MV^{2+}) was obtained from commercial sources. All the experiments were repeated at least twice.

For resistance in liquid medium, overnight cultures were diluted 100-fold into LB medium, grown to early logarithmic phase and diluted to A_{600} = 0.01 in LB medium containing 30 mM BTP, pH 7.5, and the indicated concentrations of MV^{2+} in a 96-well plate (Nunc, Roskilde, Denmark) at 37 °C with constant shaking. OD_{600} readings were taken every hour for 13 h using a Synergy 2 Microplate Reader (BioTek, Vermont, USA). The experiment was carried out in duplicate and repeated at least twice.

Generation of targeted mutations by site-directed mutagenesis

Construction of the EmrE S43A, BP A43S and TB A42S mutants was performed by PCR using QuikChange® II Site-Directed Mutagenesis Kit (Stratagene). For each mutation, a set of two overlapping oligonucleotide primers containing the desired mutation was constructed. Mutagenic oligonucleotides were prepared by incorporating or removing a unique restriction site to facilitate mutant identification. We added 1 µl of PfuUltra HF DNA polymerase to a solution containing the QuikChange® buffer, 25 ng DNA template, 125 ng of each forward and reverse primers and 300 µM dNTPs (Larova). After the PCR reaction, the parental DNA template was digested using DpnI endonuclease for the selective digestion of methylated (unmutated) template DNA (as previously described by Li and Mullins [24]). Successfully mutated DNA was identified by the loss or acquisition of the unique restriction site and was then sequenced to ensure that no other mutations occurred during the amplification process.

Expression and membrane preparation

E. coli TA15 cells carrying the pT7-7 and pGP1-2 plasmids (where pT7-7 contained the construct of interest) were grown at 30 °C in minimal medium A supplemented with 0.5% glucose, 100 µg/ml ampicillin and 50 µg/ml kanamycin. When the culture reached an A_{600} = 1.0, cultures were incubated in a water bath for 15 min at 42 °C and returned to 30 °C for 2 h. The cells were then harvested by centrifugation and washed with buffer containing 150 mM NaCl, 15 mM Tris–HCl (pH 7.5) (Na buffer) and 250 mM sucrose (Na-sucrose buffer). They were then resuspended in Na-sucrose buffer containing 14.7 mM β-mercaptoethanol, 2.5 mM $MgSO_4$, 15 µg/l culture DNase and 1 mM PMSF and were broken using a LV1 microfluidiser (Microfluidics Corporation, Massachusetts, USA) at 16 kpsi. Unbroken cells were sedimented by centrifugation and the membrane fraction was collected by ultracentrifugation at 244,717*g* for 1.5 h at 4 °C and resuspended in Na-sucrose buffer. The membranes were rapidly frozen in liquid nitrogen and stored at −70 °C.

Reconstitution into proteoliposomes

Reconstitution was performed essentially as previously described [25] by solubilizing 400 µl of membranes in 2 ml of Na buffer containing 1.5% *n*-dodecyl β-maltoside (DDM, Glycon GmbH), 0.5 mM PMSF and 15 mM β-mercaptoethanol. After removal of unsolubilized material by centrifugation (208,000*g* for 30 min at 4 °C), 20 mM imidazole was added and the His-tagged protein was incubated with Ni^{2+}-nitrilotriacetic acid (Ni-NTA) beads (Qiagen, Hilden, Germany) for 1 h at 4 °C. The beads were washed with at least 2 ml of Na buffer containing 1% *n*-octyl β-D-glucopyranoside (from Glycon GmbH), 30 mM imidazole and 15 mM β-mercaptoethanol. The protein was eluted with 500 µl of the same buffer containing 200 mM imidazole and mixed with 375 µl of 10 mg *E. coli* polar lipid extract (Avanti Inc., Alabaster, AL, USA) in Na buffer and 1.2% *n*-octyl β-D-glucopyranoside. Eluted protein and phospholipids were sonicated together in a bath-type sonicator to clarity and diluted in buffer containing 1 mM dithiothreitol and 0.19 M NH_4Cl and 15 mM Tris–HCl, pH 7.5 (for the generation of a pH gradient in the assay). After 20 min at room temperature, samples were centrifuged at 208,100*g* for 70 min, and the pellet was resuspended in 100 µl of the corresponding buffer and stored at −70 °C. Prior to the transport assay, the proteoliposomes were thawed at room temperature and sonicated lightly to clarity in a bath-type sonicator (Model G112SP1T, Laboratory Supplies Co., Inc.).

[^{3}H]Tetraphenylphosphonium binding assay

This assay was done essentially as previously described [19]. Amounts of purified proteins were determined on Coomassie-stained 16% Tricine {*N*-[2-hydroxy-1,1-bis(hydroxymethyl)ethyl]glycine} SDS/PAGE, using known amounts of the corresponding protein for calibration. Ni^{2+}-nitrilotriacetic acid beads (15 µl beads per assay) were washed twice in 0.08% DDM–Na buffer. Membranes solubilized in 0.8% DDM–Na buffer were added to the washed beads and incubated at 4 °C for 1 h.

The unbound material was discarded and the His-tagged protein bound to beads was washed three times with 0.08% DDM–Na buffer. Buffer containing 10 nM [^{3}H] tetraphenylphosphonium (TPP^+) (0.8 Ci/mmol; Vitrax) was added, and the samples were incubated for 20 min at 4 °C. Separating the beads from the supernatant by pulse centrifugation stopped the reaction.

The bead fraction was then incubated for 10 min at room temperature with 450 µl of 0.08% DDM–Na buffer containing 200 mM imidazole to release the [^{3}H]TPP^+ bound His-tagged protein from the beads. After spinning down the beads, we estimated the [^{3}H]TPP^+-associated radioactivity by liquid scintillation. In each experiment, the values obtained in a control reaction with 25 µM unlabelled TPP^+ were subtracted.

[^{14}C]MV^{2+} and [^{3}H]MPP^+ transport assay

Uptake of [^{14}C]MV^{2+} into proteoliposomes was assayed essentially as previously described [26]. The reaction was started by dilution of 2 µl of the ammonium-chloride-containing proteoliposomes into 200 µl of an ammonium-free solution containing at 25 °C, 20 µM [^{14}C]methyl viologen (8.3 mCi/mmol; ARC) or 1 µM [^{3}H]MPP^+ (0.1 Ci/mmol), 140 mM KCl, 10 mM Tricine, 5 mM $MgCl_2$ and 10 mM Tris base (calibrated to pH 8.5). At given times, the reaction was stopped by dilution with 2 ml of the same ice-cold solution, filtering through Millipore GSWP (for MV^{2+}) or Supor-200® (for MPP) filters (0.22 µm) and washing with an additional 2 ml of ice-cold solution. The radioactivity on the filters was estimated by liquid scintillation. In each experiment, the values obtained in a control reaction with 15 µM nigericin, which disrupts the proton gradient, were subtracted from all experimental points. For the determination of the kinetic parameters of BP A43S and TB A42S, MV^{2+} initial rates of transport (2 min) were measured at the indicated concentrations of MV^{2+}. K_m and V_{max} were calculated using the non-linear regression software Origin 8.6 (OriginLab).

Acknowledgements

S.S. is Mathilda Marks-Kennedy Professor of Biochemistry at the Hebrew University of Jerusalem. This work was supported by Grant 97/12 from the Israel Science Foundation.

Received 30 September 2014;
Received in revised form 19 November 2014;
Accepted 21 November 2014
Available online 3 December 2014

Keywords:
multidrug transporters;
antibiotic resistance;
ion-coupled antiporters;
EmrE;
methyl viologen

Present address: O. Sade-Falk, Department of Life Sciences, Ben Gurion University of the Negev, 8410501 Beer Sheva, Israel.

Present address: Y. Elbaz-Alon, Department of Molecular Genetics, Weizmann Institute of Science, Rehovot 76100, Israel.

References

[1] Bush K, Courvalin P, Dantas G, Davies J, Eisenstein B, Huovinen P, et al. Tackling antibiotic resistance. Nat Rev Microbiol 2011;9:894–6.
[2] Center for Disease Control. Antibiotics resistance threats in the USA, 2013. Annual Report of the CDC. USA: Centers for Disease Control; 2013.
[3] Organization WWH. Antimicrobial resistance: global report on surveillance; 2014.
[4] Piddock LJ. Multidrug-resistance efflux pumps—not just for resistance. Nat Rev Microbiol 2006;4:629–36.
[5] Nikaido H, Pages JM. Broad-specificity efflux pumps and their role in multidrug resistance of Gram-negative bacteria. FEMS Microbiol Rev 2012;36:340–63.
[6] Lomovskaya O, Zgurskaya HI, Totrov M, Watkins WJ. Waltzing transporters and "the dance macabre" between humans and bacteria. Nat Rev Drug Discov 2007;6:56–65.
[7] Fluman N, Bibi E. Bacterial multidrug transport through the lens of the major facilitator superfamily. Biochim Biophys Acta 2009;1794:738–47.
[8] Schuldiner S. EmrE, a model for studying evolution and mechanism of ion-coupled transporters. Biochim Biophys Acta 2009;1794:748–62.
[9] Omote H, Hiasa M, Matsumoto T, Otsuka M, Moriyama Y. The MATE proteins as fundamental transporters of metabolic and xenobiotic organic cations. Trends Pharmacol Sci 2006;27:587–93.
[10] Murakami S, Yamaguchi A. Multidrug-exporting secondary transporters. Curr Opin Struct Biol 2003;13:443–52.
[11] Pos KM. Drug transport mechanism of the AcrB efflux pump. Biochim Biophys Acta 2009;1794:782–93.
[12] Wong K, Ma J, Rothnie A, Biggin PC, Kerr ID. Towards understanding promiscuity in multidrug efflux pumps. Trends Biochem Sci 2014;39:8–16.
[13] Nikaido H. Multidrug resistance in bacteria. Annu Rev Biochem 2009;78:119–46.
[14] Tal N, Schuldiner S. A coordinated network of transporters with overlapping specificities provides a robust survival strategy. Proc Natl Acad Sci USA 2009;106:9051–6.
[15] Schuldiner S. What Can a Living Fossil Tell Us About Evolution and Mechanism of Ion-Coupled Transporters: The Story of Small Multidrug Transporters. In: Krämer R, editor. Ziegler C, editors. Membrane Transport Mechanism: Springer Berlin Heidelberg; 2014. p. 233–48.
[16] Yerushalmi H, Lebendiker M, Schuldiner S. EmrE, an *Escherichia coli* 12-kDa multidrug transporter, exchanges toxic cations and H^+ and is soluble in organic solvents. J Biol Chem 1995;270:6856–63.
[17] Goldberg EB, Arbel T, Chen J, Karpel R, Mackie GA, Schuldiner S, et al. Characterization of a Na^+/H^+ antiporter gene of *Escherichia coli*. Proc Natl Acad Sci USA 1987;84:2615–9.

[18] Tabor S, Richardson C. A bacteriophage T7 RNA polymerase/promoter system for controlled exclusive expression of specific genes. Proc Natl Acad Sci USA 1985;82:1074–8.
[19] Muth TR, Schuldiner S. A membrane-embedded glutamate is required for ligand binding to the multidrug transporter EmrE. EMBO J 2000;19:234–40.
[20] Ninio S, Rotem D, Schuldiner S. Functional analysis of novel multidrug transporters from human pathogens. J Biol Chem 2001;276:48250–6.
[21] Altschul SF, Madden TL, Schaffer AA, Zhang J, Zhang Z, Miller W, et al. Gapped BLAST and PSI-BLAST: a new generation of protein database search programs. Nucleic Acids Res 1997; 25:3389–402.
[22] Crooks GE, Hon G, Chandonia JM, Brenner SE. WebLogo: a sequence logo generator. Genome Res 2004;14:1188–90.
[23] Schneider TD, Stephens RM. Sequence logos: a new way to display consensus sequences. Nucleic Acids Res 1990;18: 6097–100.
[24] Li F, Mullins JI. Site-directed mutagenesis facilitated by DpnI selection on hemimethylated DNA. Methods Mol Biol 2002; 182:19–27.
[25] Brill S, Falk OS, Schuldiner S. Transforming a drug/H^+ antiporter into a polyamine importer by a single mutation. Proc Natl Acad Sci USA 2012;109:16894–9.
[26] Yerushalmi H, Mordoch SS, Schuldiner S. A single carboxyl mutant of the multidrug transporter EmrE is fully functional. J Biol Chem 2001;276:12744–8.
[27] Minato Y, Shahcheraghi F, Ogawa W, Kuroda T, Tsuchiya T. Functional gene cloning and characterization of the SsmE multidrug efflux pump from Serratia marcescens. Biol Pharm Bull 2008;31:516–9.
[28] Ninio S, Schuldiner S. Characterization of an archaeal multidrug transporter with a unique amino acid composition. J Biol Chem 2003;278:12000–5.
[29] Nasie I, Steiner-Mordoch S, Schuldiner S. New substrates on the block: clinically relevant resistances for EmrE and homologues. J Bacteriol 2012;194:6766–70.
[30] Mordoch SS, Granot D, Lebendiker M, Schuldiner S. Scanning cysteine accessibility of EmrE, an H^+-coupled multidrug transporter from *Escherichia coli*, reveals a hydrophobic pathway for solutes. J Biol Chem 1999;274:19480–6.
[31] Rotem D, Steiner-Mordoch S, Schuldiner S. Identification of tyrosine residues critical for the function of an ion-coupled multidrug transporter. J Biol Chem 2006;281:18715–22.
[32] Srinivasan VB, Rajamohan G, Gebreyes WA. Role of AbeS, a novel efflux pump of the SMR family of transporters, in resistance to antimicrobial agents in *Acinetobacter baumannii*. Antimicrob Agents Chemother 2009;53:5312–6.
[33] Chen YJ, Pornillos O, Lieu S, Ma C, Chen AP, Chang G. X-ray structure of EmrE supports dual topology model. Proc Natl Acad Sci USA 2007;104:18999–9004.
[34] Fleishman SJ, Harrington SE, Enosh A, Halperin D, Tate CG, Ben-Tal N. Quasi-symmetry in the cryo-EM structure of EmrE provides the key to modeling its transmembrane domain. J Mol Biol 2006;364:54–67.
[35] Schuldiner S. Undecided membrane proteins insert in random topologies. Up, down and sideways: it does not really matter. Trends Biochem Sci 2012;37:215–9.
[36] Jack DL, Storms ML, Tchieu JH, Paulsen IT, Saier MH. A broad-specificity multidrug efflux pump requiring a pair of homologous SMR-type proteins. J Bacteriol 2000;182:2311–3.
[37] Neyfakh AA. Mystery of multidrug transporters: the answer can be simple. Mol Microbiol 2002;44:1123–30.
[38] Nakashima R, Sakurai K, Yamasaki S, Hayashi K, Nagata C, Hoshino K, et al. Structural basis for the inhibition of bacterial multidrug exporters. Nature 2013;500:102–6.
[39] Eicher T, Cha HJ, Seeger MA, Brandstatter L, El-Delik J, Bohnert JA, et al. Transport of drugs by the multidrug transporter AcrB involves an access and a deep binding pocket that are separated by a switch-loop. Proc Natl Acad Sci USA 2012;109:5687–92.
[40] Peters KM, Brooks BE, Schumacher MA, Skurray RA, Brennan RG, Brown MH. A single acidic residue can guide binding site selection but does not govern QacR cationic-drug affinity. PLoS One 2011;6:e15974.